

## A model of the bifurcated current sheet

M. I. Sitnov,<sup>1,2</sup> P. N. Guzdar,<sup>3</sup> and M. Swisdak<sup>3</sup>

Received 27 February 2003; revised 28 April 2003; accepted 5 June 2003; published 12 July 2003.

[1] Recent Geotail and Cluster observations revealed that thin current sheets in the near-Earth tail may have a bifurcated structure. In some cases the electrons are found to dominate the current. We present a generalization of the Harris current sheet equilibrium, which reproduces these features. The model ion distribution contains an additional element, viz. the quasi-adiabatic invariant of the ion motion across the sheet, and assumes ion temperature anisotropy outside the sheet. Bifurcated current sheets appear in the case of small ion anisotropy with  $T_{\perp i} > T_{\parallel i}$  (pancake distributions). In the opposite case (cigar distributions) the model describes a single-peaked ion-dominated current sheet embedded in a thicker Harris sheet, which is more relevant to the outflow region of the collisionless reconnection pattern in the deHoffman-Teller frame. **INDEX TERMS:** 2744 Magnetospheric Physics: Magnetotail; 7827 Space Plasma Physics: Kinetic and MHD theory; 7835 Space Plasma Physics: Magnetic reconnection. **Citation:** Sitnov, M. I., P. N. Guzdar, and M. Swisdak, A model of the bifurcated current sheet, *Geophys. Res. Lett.*, 30(13), 1712, doi:10.1029/2003GL017218, 2003.

### 1. Introduction

[2] Studies of the geomagnetotail current sheet (CS) using two closely located spacecraft [Fairfield, 1984; McPherron *et al.*, 1987; Sergeev *et al.*, 1993] revealed that its thickness  $L$  may be as small as the thermal ion gyro-radius  $\rho_{0i}$  in the field outside. In such sheets the ions are nonadiabatic and electron and ion dynamics become decoupled, resulting in many new effects. In particular, the thin current sheet (TCS) may be embedded in a thicker plasma sheet [e.g., McComas *et al.*, 1986]. Also, the current density in the TCS may be dominated by electrons [Mukai *et al.*, 1998].

[3] One of the most recent findings is the explicit demonstration that the CS may have a bifurcated structure with two current density peaks separated by a current depression region at the sheet center [Nakamura *et al.*, 2002; Runov *et al.*, 2003; Sergeev *et al.*, 2003]. These results have been obtained using four spacecraft Cluster observations, which allowed, for the first time, the unambiguous separation of spatial and temporal variability. They confirmed previous single event observations of bifurcated current sheets made using the ISEE 1 and 2 spacecraft [Sergeev *et al.*, 1993] and the single-spacecraft Geotail

observations [Hoshino *et al.*, 1996; Asano, 2001]. An important additional feature of the new TCS observations was a very small (less than a few nT) dawn-dusk component of the magnetic field making it hard to explain the bifurcated structure in terms of electron-dominated currents near an X-line [Arzner and Scholer, 2001]. The bifurcated structure was stable in spite of the fast flapping motions of the CS as a whole [Sergeev *et al.*, 2003].

[4] These new features demand a considerable modification and extension of the standard CS models based on the Harris equilibrium [Harris, 1962]. One such modification [Sitnov *et al.*, 2000a, 2000b] has been proposed in the form of a new class of ion-dominated TCS equilibria, where the ion current is formed mainly by the quasi-adiabatic serpentine motion of ions [Speiser, 1965]. A distinctive feature of the model was the use of the new quasi-adiabatic invariant of the ion motion across the sheet [Sonnerup, 1971] in place of the dawn-dusk component of the canonical momentum used in Harris-type models. Another class of TCS models proposed recently by Schindler and Birn [2002] is based on a generalization of the Harris approach, which assumes non-Maxwellian distributions, but retains the original set of integrals of motion.

[5] In this letter we propose a generalization of the Harris approach by combining it with that of Sitnov *et al.* [2000a, 2000b]. It is shown that the generalized model describes the bifurcated current sheets (hereafter BCS). It also describes both ion- and electron-dominated TCS.

### 2. Basic Equations

[6] The model is based on a set of Ampère's and Poisson's equations, of which the latter is reduced to the quasi-neutrality condition

$$\frac{dB_x}{dz} = \sum_{\alpha=e,i} \frac{4\pi q_\alpha}{c} \int v_y f_{0\alpha}(z, \mathbf{v}) d^3v \quad (1)$$

$$\int f_{0i}(z, \mathbf{v}) d^3v = \int f_{0e}(z, \mathbf{v}) d^3v \quad (2)$$

The electron and ion distributions have the form

$$f_{0\alpha} \propto \exp\left(-\frac{2W_\alpha - \omega_{0\alpha} I_z^{(\alpha)}}{2T_{\parallel\alpha}} + \frac{v_{D\alpha} P_{y\alpha}}{T_{\parallel\alpha}} - \frac{\omega_{0\alpha} I_z^{(\alpha)}}{2T_{\perp\alpha}}\right), \quad (3)$$

where  $T_{\parallel\alpha}$ ,  $T_{\perp\alpha}$ ,  $\omega_{0\alpha} = eB_0/m_\alpha c$  ( $e = |q_\alpha|$ ), and  $v_{D\alpha}$  are the parallel and perpendicular temperatures, the cyclotron frequency, and constant speed parameter for the species  $\alpha$ , respectively;  $\alpha = e, i$ , and  $B_0$  is the magnetic field outside the sheet. They are constructed from three integrals of motion. The first two, namely the total particle energy  $W_\alpha = m_\alpha v^2/2 + q_\alpha \phi$  ( $\phi$  is the electrostatic potential) and the out-of-plane (dawn-dusk) component of the canonical momentum

<sup>1</sup>Department of Astronomy, University of Maryland, College Park, Maryland, USA.

<sup>2</sup>Also at Skobel'syn Institute of Nuclear Physics, Moscow State University, Moscow, Russia.

<sup>3</sup>Institute for Research in Electronics and Applied Physics, University of Maryland, College Park, Maryland, USA.

$P_{y\alpha} = m_\alpha v_y + (q_\alpha/c) A_y$  are those used in the Harris model. We extend this set of invariants by including the quasi-adiabatic invariant of the particle motion across the sheet [Sonnerup, 1971]

$$I_z^{(\alpha)} = \frac{1}{2\pi} \oint m_\alpha v_z dz \quad (4)$$

This is an exact invariant of the particle motion in the case of zero normal component of the magnetic field  $B_n$ . Moreover, even for  $B_n \neq 0$  it remains approximately constant for ions in a TCS with  $L \sim \rho_{0i}$  as long as  $B_n \ll B_0$  (for details see [Sitnov et al., 2000a] and refs. therein). In that case the electron invariant  $I_z^{(e)}$  can be modified to form the conventional magnetic moment.  $I_z^{(\alpha)}$  becomes essential, in particular, for the case of the temperature anisotropy,  $T_{\parallel\alpha} \neq T_{\perp\alpha}$ , outside the sheet.

[7] In the region  $z \geq 0$  the expression for  $I_z^{(\alpha)}$  can be re-written explicitly as

$$I_z^{(\alpha)} = \frac{2m_\alpha}{\pi} \int_{z_0}^{z_1} dz' \sqrt{W_1^2(v_y, v_z, z, z') - W_2^2(v_y, z, z')}, \quad (5)$$

where  $W_1 = \sqrt{v_y^2 + v_z^2 + (2q_\alpha/m_\alpha)[\phi(z) - \phi(z')]}$ ,  $W_2 = v_y + (q_\alpha/m_\alpha c) \int_{z'}^z B_x(z'') dz''$ , and the limits of the integration are given by the equation

$$W_2(v_y, z, z_{0,1}) \pm W_1(v_y, v_z, z, z_{0,1}) = 0 \quad (6)$$

with  $z_0 < z < z_1$  and the additional restriction that  $z_0 = 0$  if the formal solution of (6) becomes negative. For electrons, these expressions can be simplified in the main part of the sheet because  $\rho_{0e} \ll L \sim \rho_{0i}$ . Expanding the electrostatic potential and magnetic field around the point  $z$  we obtain, instead of (5), the expression  $I_z^{(e)} = (m_e/\omega_{Be}) [v_z^2 + (v_y - v_E)^2]$ , which is proportional to the magnetic moment in the case  $B_n = 0$ . Here  $v_E = cE_z(z)/B(z)$  and  $\omega_{Be} = eB(z)/m_e c$  are the drift velocity in the crossed fields  $\mathbf{E}_z \times \mathbf{B}$  and the particle gyrofrequency, respectively. It is important to note that though  $I_z^{(e)}$  describes the  $\mathbf{E}_z \times \mathbf{B}$  drift, the velocity space integral in (1) yields a more complicated expression for the electron bulk flow speed than  $v_E$ .

[8] In the limit  $T_{\parallel} = T_{\perp}$  the distribution (3) takes the classical isotropic form [Harris, 1962]. In another limiting case,  $v_{D\alpha} = 0$  and  $T_{\parallel} > T_{\perp}$ , it becomes cigar-like and resembles the counterstreaming ion distribution of the forced current sheet model [Sitnov et al., 2000a, 2000b]. Below we consider a more general case  $v_{D\alpha} \neq 0$  and  $T_{\parallel i} \neq T_{\perp i}$ . The distribution (3), which is used below

$$\begin{aligned} f_{0\alpha} &= \frac{\delta_\alpha n_0}{\pi^{3/2} v_{T\parallel\alpha}^2 v_{T\perp\alpha}^2} \exp\left(\frac{q_\alpha v_{D\alpha}}{c T_{\parallel\alpha}} A_y - \frac{q_\alpha \phi}{T_{\parallel\alpha}}\right) \\ &\times \exp\left\{-\frac{m_\alpha}{2 T_{\parallel\alpha}} \left[v_x^2 + (v_y - v_{D\alpha})^2 + v_z^2\right]\right\} \\ &\times \exp\left[\left(T_{\parallel\alpha}^{-1} - T_{\perp\alpha}^{-1}\right) \frac{\omega_{0\alpha}}{2} I_z^{(\alpha)}\right] \end{aligned} \quad (7)$$

with  $\delta_\alpha = \exp[-(v_{D\alpha}^2/v_{T\parallel\alpha}^2)(T_{\perp\alpha}/T_{\parallel\alpha} - 1)]$ ,  $v_{T\parallel\alpha} = \sqrt{2T_{\parallel\alpha}/m_\alpha}$  and  $v_{T\perp\alpha} = \sqrt{2T_{\perp\alpha}/m_\alpha}$ , yields the Harris profile outside the sheet ( $|z| \gg \rho_{0i}$ ) where  $I_z^{(\alpha)} \rightarrow (2m_\alpha c/e) M^{(\alpha)}$  ( $M^{(\alpha)}$  is the magnetic moment) with the bulk flow speed in the Y-direction  $v_{D\alpha}^{(0)} = v_{D\alpha}(T_{\perp\alpha}/T_{\parallel\alpha})$ .

[9] Now we introduce a number of dimensionless parameters and variables. The group of fixed parameters includes the temperature ratio  $\tau = T_{\perp e}/T_{\parallel e}$ , the anisotropy ratio  $\eta_\alpha = T_{\perp\alpha}/T_{\parallel\alpha}$ , the mass ratio  $\mu = m_e/m_i$ , and the dimensionless drift speed  $w_{D\alpha} = v_{D\alpha}/v_{T\perp\alpha}$ . The parameter to be determined as a result of the solution of the equilibrium equations is the effective plasma beta  $\beta_0 = 8\pi n_0 T_{\perp i}/B_0^2$ , which characterizes the compression of the sheet. We also normalize the magnetic field  $b = B_x/B_0$ , the electromagnetic potential  $A_y = -aB_0\rho_{\perp 0i}$  (where  $a = \int^\zeta b(\zeta') d\zeta'$  with  $\zeta = z/\rho_{\perp 0i}$ ,  $\rho_{\perp 0i} = v_{T\perp i}/\omega_{0i}$ ), the electrostatic potential  $\phi = T_{\perp i}\varphi/e$ , the spatial coordinate  $z = \rho_{\perp 0i}\zeta$ , the particle velocity  $v_{y,z} = v_{\perp T\alpha} w_{y,z}$ , and the invariant  $I_z^{(\alpha)} = I^{(\alpha)} m_\alpha v_{T\perp\alpha} \rho_{\perp 0\alpha}$ . Furthermore, we transform Ampère's equation (1) into an integral equation for the function  $b(a) = b(\zeta(a))$  by changing variables  $\zeta \rightarrow a$  and using the identity  $db/d\zeta = (db/da)(da/d\zeta) = (1/2)(db^2/da)$ . Finally, we limit the consideration below to the case of isotropic electron species. Then Ampère's equation can be written as

$$b(a) = \sqrt{2\beta_0(P_i(a) + P_e(a))}, \quad (8)$$

where

$$\begin{aligned} P_i &= \pi^{-1} \exp[-w_{Di}^2 \eta_i (\eta_i - 1)] \int_0^a da' \exp(-2\eta_i w_{Di} a') \\ &\times \exp(-\eta_i \varphi) \int w_y dw_y dw_z F(w_y, w_z, a') \end{aligned} \quad (9)$$

with  $F = \exp((\eta_i - 1) I^{(i)} - \eta_i (w_y - w_{Di})^2 - \eta_i w_z^2)$  and

$$P_e = -\tau^{1/2} \mu^{-1/2} w_{De} \int_0^a da' \exp(2w_{De} \tau^{-1/2} \mu^{-1/2} a' + \tau^{-1} \varphi) \quad (10)$$

The quasi-adiabatic invariant  $I^{(i)}$  is given by the formula

$$\begin{aligned} I^{(i)}(a', w_y, w_z) &= \frac{2}{\pi} \int_{a_0}^{a_1} \frac{da''}{b(a'')} \\ &\times \sqrt{w_y^2 + w_z^2 + [\varphi(a') - \varphi(a'')] - [w_y + a'' - a']^2}, \end{aligned} \quad (11)$$

where  $a_{0,1} = a' - w_y \mp \sqrt{w_y^2 + w_z^2 + [\varphi(a') - \varphi(a_{0,1})]}$ , if  $0 < a_0 < a < a_1$  and  $a_0 = 0$  if the formal solution for  $a_0$  becomes negative.

[10] The quasi-neutrality equation takes the form

$$\begin{aligned} \varphi(\tau^{-1} + \eta_i) &= \log\left\{\pi^{-1} \int dw_y dw_z F(w_y, w_z, a)\right\} \\ &- w_{Di}^2 \eta_i (\eta_i - 1) - 2a(w_{De} \tau^{-1/2} \mu^{-1/2} + \eta_i w_{Di}) \end{aligned} \quad (12)$$

The system (8)–(12) is complemented by the condition  $w_{De} \tau^{-1/2} \mu^{-1/2} + \eta_i w_{Di} = 0$ , which provides neutrality outside the sheet and transforms into the well-known relation  $v_{Di}/v_{De} = -T_i/T_e$  in the case of the Harris CS.

### 3. Solution of the Equilibrium Equations

[11] The solution of the equilibrium equations (8)–(12) represents a nonlinear eigenvalue problem for the functions  $b(a)$ ,  $\varphi(a)$ , and the unknown parameter  $\beta_0$ . It can be iteratively solved starting from the Harris equilibrium for

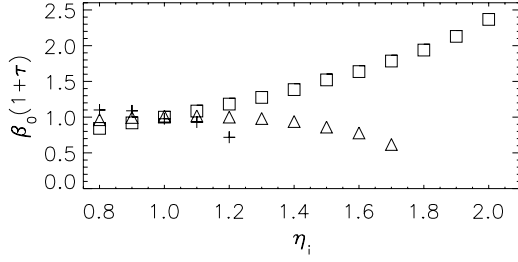


**Figure 1.** Values of the parameter  $\beta_0$  found as solutions of the equilibrium equations (8)–(12) for different values of anisotropy  $\eta_i$  and the Harris part of the ion bulk flow velocity  $w_{Di} = 0.125$  (+),  $0.25$  ( $\triangle$ ), and  $0.5$  ( $\square$ ).

the parameters  $\tau = 1/4$  and  $\mu = 1/1836$  (for details of the numerical technique see [Sitnov *et al.*, 2000a, 2000b] and refs. therein). The eigenvalues  $\beta_0$  are shown in Figure 1 as functions of the parameter  $\eta_i$  for different values of the drift velocity  $w_{Di}$ . All the curves converge at the point  $\eta_i = 1$  (isotropic plasma) with  $\beta_0(1 + \tau) = 1$ , which corresponds to the well known relation of the Harris model  $B_0^2 = 8\pi n_0(T_i + T_e)$ . The eigenfunctions in the form of the profiles of the magnetic field  $b(\zeta)$ , electrostatic potential  $\varphi(\zeta)$ , plasma density  $n(\zeta)$  and current density  $J(\zeta)$  are shown in Figures 2–4. In particular, Figure 2 shows these profiles for the cigar ion distribution with the parameters  $\eta_i = 0.8$  and  $w_{Di} = 0.125$ . They reproduce the positive charging and embedding within the thicker plasma sheet, that is the distinctive features of the TCS formed by counter-streaming field-aligned ion flows and known as the forced CS ([Sitnov *et al.*, 2000a, 2000b] and refs. therein). However, in contrast to the earlier models, the thicker plasma sheet is now the conventional Harris CS rather than a background plasma with a constant density and zero current.

[12] The formation of BCS becomes possible for pancake ion distributions ( $T_{\perp i} > T_{\parallel i}$ ) outside the sheet. Note that this type of the ion anisotropy is a natural consequence of the

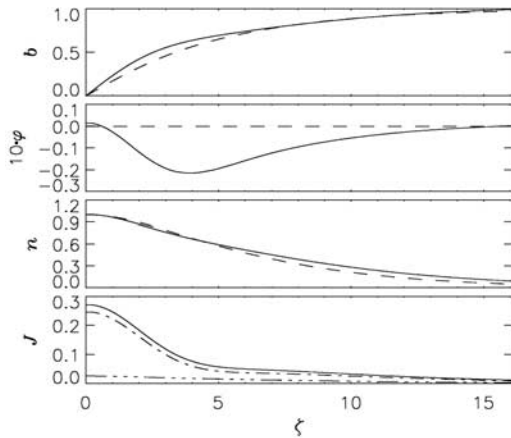


**Figure 2.** Profiles of the magnetic field  $b(\zeta)$ , electrostatic potential  $\varphi(\zeta)$ , plasma density  $n(\zeta)$ , and current density  $J(\zeta)$  found for the parameters  $\eta_i = 0.8$  (cigar distribution) and  $w_{Di} = 0.125$ . Dashed lines show the corresponding profiles of the Harris sheet. Dash-dotted and dash-triple dotted lines show the contributions to the current density of ion and electron species, respectively.

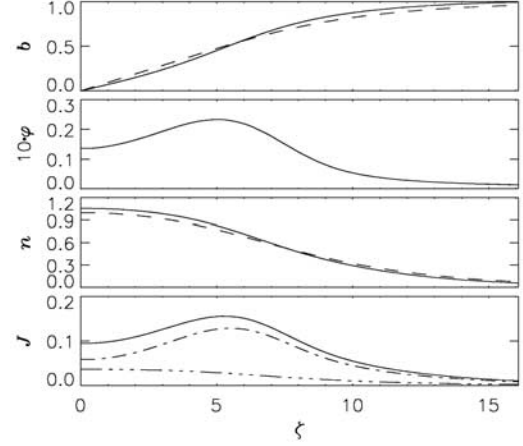


**Figure 3.** Profiles described in Figure 2 shown for the case of the pancake ion distribution outside the sheet with the parameters  $\eta_i = 1.1$  and  $w_{Di} = 0.125$ .

CS compression by the convection dawn-dusk electric field  $E_y$ , although this field itself cannot be included in the present equilibrium model. Since the ions spread out across the whole plasma sheet instead of following the electron convection flow toward the CS [Pritchett and Coroniti, 1995], the energy going into this species will dominantly heat it. However, this heating will first affect the perpendicular component of the ion velocity because of the small normal component  $B_n \ll B_0$  of the CS magnetic field (in the limit  $B_n = 0$  the parallel component of the velocity is an integral of motion even for the case  $E_y \neq 0$ ). It is interesting to note that Lui *et al.* [1992] found pancake proton distributions with  $\eta_i = 1.04$ – $1.34$  prior to all current disruption events studied using the AMPTE CCE spacecraft. Figure 3 shows that even a small (10%) pancake anisotropy of the ions outside the CS drastically modifies the Harris sheet profile, transforming it into a BCS (bottom panel). It also shows a considerable increase of the electron contribution to the total current density at the center of the sheet, which is provided however mainly because of the reduction of the corresponding ion contribution. Further increase of the

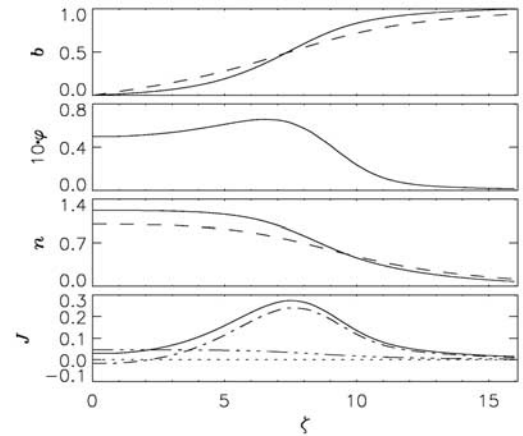


**Figure 4.** Profiles described in Figure 2 for the case of electron current domination at the center of the BCS ( $\eta_i = 1.2$  and  $w_{Di} = 0.125$ ).

anisotropy results in the domination of the electron current in the central CS region as is seen in Figure 4. Note that while the electron current density exceeds the ion density at the center of the sheet, the two off-center peaks are still due to the ions. Thus, the drift of electrons in the crossed fields  $E_z = -\partial\phi/\partial z$  and  $B$  is not the main mechanism for maintaining the equilibrium BCS, but that may be the case during its formation by the convection field  $E_y$  [Pritchett and Coroniti, 1995; Hesse et al., 1998]. Although the central part of the equilibrium BCS is negatively charged as compared to the region of the maximum current density, the latter region is closer to the peak of the potential rather than its  $z$ -derivative as would be the case for currents dominated by the  $\mathbf{E}_z \times \mathbf{B}$  drift.

[13] Signatures of the current bifurcation were found earlier in a number of numerical TCS models with various ion source distributions [Holland and Chen, 1995; Harold and Chen, 1996] including those of trapped ions [Zelenyi et al., 2002]. Interestingly, the abundance of trapped ions and pancake anisotropy may have similar effects on the CS structure as both phenomena imply the domination of ions with large values of the invariant  $I_z^{(i)}$ . And yet, the BCS solution found in our model cannot be explained by the dynamics of the quasi-adiabatic ions and in particular its trapped component alone. It forms as a result of the balance between the features of the quasi-adiabatic ion motion (due to the new invariant  $I_z^{(i)}$ ) and those of the Harris part of the CS. We find, in particular, no BCS solutions in the limit  $w_{Di} \rightarrow 0$ , where the Harris constituent is sufficiently small.

[14] Another distinctive feature of the present BCS model, which is consistent with observations [Sergeev et al., 2003], is the formation of a plateau in the profile of the plasma density in the central CS region between the current peaks (Figure 4). This effect is particularly well seen when compared to the pure Harris profile (dashed line in Figure 4). One distinctive feature of the model, namely the ion current density domination in the peak regions, seems to be at variance with observations, which display no such features yet. It should be noted however, that a similar characteristic profile of the ion current (in the form of an inverted “W”) was reported by Pritchett and Coroniti [1995] whereas the simulated electron current did not show any such feature.

[15] With further increase of the anisotropy  $\eta_i$  for the drift speeds  $w_{Di} = 0.125$  and  $0.25$  the total current density at the center of the sheet becomes negative and a self-consistent equilibrium vanishes. On the other hand, with the increase of the dimensionless ion drift velocity  $w_{Di}$ , the total thickness of the CS approaches the ion gyroradius  $\rho_{0i}$  but the BCS structure disappears. An interesting and yet unexplained feature of this case is the qualitatively different behavior of the parameter  $\beta_0$  as a function of anisotropy  $\eta_i$  (Figure 1).

#### 4. Conclusion

[16] We have shown that the generalization of the Harris CS model assuming ion anisotropy outside the CS and taking into account the quasi-adiabatic properties of the ion serpentine motion, gives rise to a large family of TCS equilibria, which describe such distinctive features as their characteristic scales, domination of either ion or electron species in the current production, embedding, and bifurcated structures. In particular, the model reproduces the double-peaked structure

of the current density and the plateau of the plasma density in the current depression region. Thus it can be used for comparison with the observed BCS along with the slow shock [Hoshino et al., 1996] and electron-dominated CS [Hesse et al., 1998; Arzner and Scholer, 2001] models.

[17] **Acknowledgments.** We are grateful to V. Sergeev, A. Runov and W. Baumjohann for bringing our attention to the recent Cluster observations of bifurcated current sheets and stimulating this research. We also thank M. Hoshino and Y. Asano for similar stimulating information based on Geotail observations. The work was supported by NASA under contracts NAG510298 and NAG513047.

#### References

- Arzner, K., and M. Scholer, Kinetic structure of the post plasmoid plasma sheet during magnetic reconnection, *J. Geophys. Res.*, **106**, 3827, 2001.
- Asano, Y., Configuration of the thin current sheet in substorms, PhD Thesis, Univ. of Tokyo, 2001.
- Fairfield, D. H., Magnetotail energy storage and the variability of the magnetotail current sheet, in *Magnetic Reconnection in Space and Laboratory Plasmas*, Geophys. Monogr. Ser., vol. 30, edited by E. W. Hones, p. 168, AGU, Washington, D. C., 1984.
- Harris, E. G., On a plasma sheath separating regions of oppositely directed magnetic fields, *Nuovo Cimento*, **23**, 115, 1962.
- Harold, J. B., and J. Chen, Kinetic thinning in one-dimensional self-consistent current sheets, *J. Geophys. Res.*, **101**, 24,899, 1996.
- Hesse, M., et al., On the ion-scale structure of thin current sheets in the magnetotail, *Phys. Scripta*, **T74**, 63, 1998.
- Holland, D. L., and J. Chen, Kinetic current sheet equilibria in the quiet-time magnetotail, in *Physics of Space Plasmas (1993)*, No.13, edited by T. Chang and J. R. Jasperse, p. 281, Mass. Inst. of Technol. Cent. for Theor. Geo/Cosmo Plasma Phys., Cambridge, 1995.
- Hoshino, M., et al., Structure of plasma sheet in magnetotail: Double-peaked electric current sheet, *J. Geophys. Res.*, **101**, 24,775, 1996.
- Lui, A. T. Y., et al., Current disruptions in the near-Earth neutral sheet region, *J. Geophys. Res.*, **97**, 1461, 1992.
- McComas, D. J., et al., The near-earth cross-tail current sheet: Detailed ISEE 1 and 2 case studies, *J. Geophys. Res.*, **91**, 4287, 1986.
- McPherron, R. L., et al., Is near-Earth current sheet thinning the cause of auroral substorm onset? in *Quantitative Modeling of Magnetosphere-Ionosphere Coupling Processes*, edited by Y. Kamide and R. A. Wolf, p. 252, Kyoto Sangyo University, Kyoto, Japan, 1987.
- Mukai, T., et al., Pre-onset and onset signatures for substorms in the near-tail plasma sheet: GEOTAIL observations, in *SUBSTORMS-4*, edited by S. Kokubun and Y. Kamide, Terra Scientific Publ. Co./Kluwer Academic Publishers, 131, 1998.
- Nakamura, R., et al., Fast flows during current sheet thinning, *Geophys. Res. Lett.*, **29**(23), 2140, doi:10.1029/2002GL016200, 2002.
- Pritchett, P. L., and F. V. Coroniti, Formation of thin current sheets during plasma sheet convection, *J. Geophys. Res.*, **100**, 23,551, 1995.
- Runov, A., et al., Cluster observations of a bifurcated current sheet, *Geophys. Res. Lett.*, **30**(2), 1036, doi:10.1029/2002GL016136, 2003.
- Schindler, K., and J. Birn, Models of two-dimensional embedded thin current sheets from Vlasov theory, *J. Geophys. Res.*, **107**(A8), 10.1029/2001JA000304, 2002.
- Sergeev, V. A., et al., Structure of the tail plasma/current sheet at 11 Re and its changes in the course of a substorm, *J. Geophys. Res.*, **98**, 17,345, 1993.
- Sergeev, V., et al., Flapping motions and current sheet structure during substorm activation as observed by Cluster, *Geophys. Res. Lett.*, **30**(6), 1327, doi:10.1029/2002GL016500, 2003.
- Sitnov, M. I., et al., Thin current sheet embedded within a thicker plasma sheet: Self-consistent kinetic theory, *J. Geophys. Res.*, **105**, 13,029, 2000a.
- Sitnov, M. I., et al., Distinctive features of forced current sheets: Electrostatic effects, in *Proc. 5th Int. Conf. on Substorms (ICS-5)*, St. Petersburg, Russia 16–20 May 2000, ESA SP-443, p. 197, 2000b.
- Sonnerup, B. U. Ö., Adiabatic particle orbits in a magnetic null sheet, *J. Geophys. Res.*, **76**, 8211, 1971.
- Speiser, T. W., Particle trajectories in model current sheets, 1, Analytical solutions, *J. Geophys. Res.*, **70**, 4219, 1965.
- Zelenyi, L. M., et al., Catastrophic-like evolution of thin current sheets due to non-adiabatic scattering processes, in *Proc. 6th Int. Conf. on Substorms*, 25–29 March, Seattle, p. 245, 2002.

M. I. Sitnov, Department of Astronomy, University of Maryland, College Park 20742, USA. (sitnov@astro.umd.edu)

P. N. Guzdar and M. Swisdak, Institute for Research in Electronics and Applied Physics, University of Maryland, College Park 20742, USA.